

A pan-African high-resolution drought index dataset

Jian Peng^{1,2}, Simon Dadson¹, Feyera Hirpa¹, Ellen Dyer¹, Thomas Lees¹, Diego G. Miralles³, Sergio M. Vicente-Serrano⁴, Chris Funk^{5,6}

1. School of Geography and the Environment, University of Oxford, OX1 3QY Oxford, UK;

2. Max Planck Institute for Meteorology, Hamburg, Germany;

3. Hydro-Climatic Extremes Lab (H-CEL), Ghent University, Ghent, Belgium;

4. Instituto Pirenaico de Ecología, Consejo Superior de Investigaciones Científicas (IPE-CSIC) Zaragoza, Spain;

5. U.S. Geological Survey, Earth Resources Observation and Science Center, Sioux Falls, South Dakota;

6. Santa Barbara Climate Hazards Center, University of California, USA;

Corresponding author: Jian Peng (jian.peng@ouce.ox.ac.uk)

Abstract

Droughts in Africa cause severe problems such as crop failure, food shortages, famine, epidemics and even mass migration. To minimize the effects of drought on water and food security over Africa, a high-resolution drought dataset is essential to establish robust drought hazard probabilities and to assess drought vulnerability considering a multi- and cross-sectorial perspective that includes crops, hydrological systems, rangeland, and environmental systems. Such assessments are essential for policy makers, their advisors, and other stakeholders to respond to the pressing humanitarian issues caused by these environmental hazards. In this study, a high spatial resolution Standardized Precipitation-Evapotranspiration Index (SPEI) drought dataset is presented to support these assessments. We compute historical SPEI data based on Climate Hazards group InfraRed Precipitation with Station data (CHIRPS) precipitation estimates and Global Land Evaporation Amsterdam Model (GLEAM) potential evaporation estimates. The high resolution SPEI dataset (SPEI-HR) presented here spans from 1981 to 2016 (36 years) with 5 km spatial resolution over the whole Africa. To facilitate the diagnosis of droughts of different durations, accumulation periods from 1 to 48 months are provided. The quality of the resulting dataset was compared with coarse-resolution SPEI based on Climatic Research Unit (CRU) Time-Series (TS) datasets, and Normalized Difference Vegetation Index (NDVI) calculated from the Global Inventory Monitoring and Modeling System (GIMMS) project, as well as with root zone soil moisture modelled by GLEAM. Agreement found between coarse resolution SPEI

30 from CRU TS (SPEI-CRU) and the developed SPEI-HR provides confidence in the estimation of temporal
31 and spatial variability of droughts in Africa with SPEI-HR. In addition, agreement of SPEI-HR versus NDVI
32 and root zone soil moisture – with average correlation coefficient (R) of 0.54 and 0.77, respectively – further
33 implies that SPEI-HR can provide valuable information to study drought-related processes and societal
34 impacts at sub-basin and district scales in Africa. The dataset is archived in Centre for Environmental Data
35 Analysis (CEDA) with link: <http://dx.doi.org/10.5285/bbdfd09a04304158b366777eba0d2aeb> (Peng et al.,
36 2019a)

37 **Keywords:**

38 Drought, Africa, Precipitation, Potential evaporation, drought management, disaster risk reduction

39
40
41
42
43
44
45
46
47
48
49
50
51
52
53
54
55
56
57
58
59
60

61 **1 Introduction**

62 Drought is a complex phenomenon that affects natural environments and socioeconomic systems in the
63 world (von Hardenberg et al., 2001; Vicente-Serrano, 2007; Van Loon, 2015; Wilhite and Pulwarty, 2017).
64 Impacts include crop failure, food shortage, famine, epidemics and even mass migration (Wilhite et al.,
65 2007; Ding et al., 2011; Zhou et al., 2018). In recent years, severe events have occurred across the world,
66 such as the 2003 central Europe drought (García-Herrera et al., 2010), the 2010 Russian drought (Spinoni et
67 al., 2015), the 2011 Horn of Africa drought (Nicholson, 2014), the southeast Australian's Millennium
68 drought (van Dijk et al., 2013; Peng et al., 2019d), the 2013/2014 California drought (Swain et al., 2014), the
69 2014 North China drought (Wang and He, 2015) and the 2015–2017 Southern Africa drought (Baudoin et
70 al., 2017; Muller, 2018). Widespread negative effects of these droughts on natural and socioeconomic
71 systems have been reported afterwards (Wegren, 2011; Arpe et al., 2012; Griffin and Anchukaitis, 2014;
72 Mann and Gleick, 2015; Dadson et al., 2019; Marvel et al., 2019). Thus, there is a clear need to improve our
73 knowledge about the spatial and temporal variability of drought, which provides a basis for quantifying
74 drought impacts and the exposure of society, the economy and the environment over different areas and
75 time-scales (Pozzi et al., 2013; AghaKouchak et al., 2015).

76 Generally, drought is defined as a temporal anomaly characterized by a deficit of water compared with long-
77 term conditions (Mishra and Singh, 2010; Van Loon, 2015). Droughts can typically be grouped into five
78 types: meteorological (precipitation deficiency), agricultural (soil moisture deficiency), hydrological (runoff
79 and/or groundwater deficiency), socioeconomic (social response to water supply and demand) and
80 environmental or ecologic (Keyantash and Dracup, 2002; AghaKouchak et al., 2015; Crausbay et al., 2017).
81 These different drought categories involve different event characteristics in terms of timing, intensity,
82 duration, and spatial extent, making it very difficult to characterize droughts quantitatively (Panu and
83 Sharma, 2002; Lloyd-Hughes, 2014; Vicente-Serrano, 2016). For this reason numerous drought indices have
84 been proposed for precise applications, and reviews of the available indices have been provided by previous
85 studies such as Heim Jr (2002), Keyantash and Dracup (2002), and Mukherjee et al. (2018). Van Loon

86 (2015) noted that there is no best drought index for all types of droughts, because every index is designed for
87 a specific drought type, thus multiple indices are required to capture the multifaceted nature of drought.
88 Nevertheless, the Standardized Precipitation Index (SPI) is recommended by the World Meteorological
89 Organization (WMO) for drought monitoring, which is calculated based solely on long-term precipitation
90 data over different time spans (McKee et al., 1993). The advantages of SPI are its relative simplicity and its
91 ability to characterize different types of droughts given the different times of response of different usable
92 water sources to precipitation deficits (Kumar et al., 2016; Zhao et al., 2017). However, information on
93 precipitation is inadequate to characterize drought; in most definitions, drought conditions also depend on
94 the demand of water vapor from the atmosphere. More recently, Vicente-Serrano et al. (2010) proposed an
95 alternative drought index for SPI, which is called Standardized Precipitation Evapotranspiration Index
96 (SPEI). Compared to SPI, it considers not only the precipitation supply, but also the atmospheric evaporative
97 demand (Beguería et al., 2010; Vicente-Serrano et al., 2012b). This makes the index more informative of the
98 actual drought effects over various natural systems and socioeconomic sectors (Vicente-Serrano et al., 2012b;
99 Bachmair et al., 2016; Kumar et al., 2016; Sun et al., 2016c; Bachmair et al., 2018; Peña-Gallardo et al.,
100 2018a; Peña-Gallardo et al., 2018b; Sun et al., 2018).

101 For the calculation of SPEI, high-quality and long-term observations of precipitation and atmospheric
102 evaporative demand are necessary. These observations may either come from ground-based station data or
103 gridded data such as satellite and reanalysis datasets. For example, the SPEIbase (Beguería et al., 2010) and
104 the Global Precipitation Climatology Centre Drought Index (GPCC-DI) (Ziese et al., 2014) both provide
105 SPEI datasets at global scale. The SPEIbase provides gridded SPEI with a 50-km spatial resolution, and is
106 calculated from Climatic Research Unit (CRU) Time-Series (TS) datasets, which are produced based on
107 measurements from more than 4000 ground-based weather stations over the world (Harris et al., 2014). The
108 SPEI dataset provided by GPCC-DI has spatial resolution of 1°, and was generated from GPCC precipitation
109 (Becker et al., 2013; Schneider et al., 2016) and National Oceanic and Atmospheric Administration
110 (NOAA)'s Climate Prediction Center (CPC) temperature dataset (Fan and Van den Dool, 2008). Both of

111 these datasets have been applied for various drought related studies at global and regional scales (e.g., Chen
112 et al., 2013; Vicente-Serrano et al., 2013; Isbell et al., 2015; Sun et al., 2016a; Vicente-Serrano et al., 2016;
113 Deo et al., 2017). However, these global SPEI data sets' spatial resolution are too coarse to be applied at
114 district or sub-basin scales (Vicente-Serrano et al., 2017). A sub-basin scale quantification of drought
115 conditions is particularly crucial in regions such as Africa, in which geospatial data and drought indices can
116 be essential to manage existing drought-related risks (Vicente-Serrano et al., 2012a) and where in-situ
117 measurements are scarce (Trambauer et al., 2013; Masih et al., 2014; Anghileri et al., 2019). Over last
118 century, Africa has been severely influenced by intense drought events, which has led to food shortages and
119 famine in many countries (Anderson et al., 2012; Yuan et al., 2013; Sheffield et al., 2014; Awange et al.,
120 2016; Funk et al., 2018; Nicholson, 2018; Gebremeskel et al., 2019). Therefore, the availability of a high-
121 resolution drought index dataset may contribute to an improved characterization of drought risk and
122 vulnerability, and minimize its impact on water and food security by supporting policy makers, water
123 managers and stakeholders. Conveniently, with the advancement of satellite technology, the estimation of
124 precipitation and evaporation from remote sensing datasets is becoming more accurate (Fisher et al., 2017).
125 In particular, the long-term Climate Hazards group InfraRed Precipitation with Station data (CHIRPS) (Funk
126 et al., 2015a) precipitation and Global Land Evaporation Amsterdam Model (GLEAM) (Miralles et al., 2011)
127 evaporation datasets provide high-quality datasets for near-real time drought monitoring. Here, we use
128 CHIRPS and GLEAM datasets to develop a pan-African high spatial resolution (5-km) SPEI dataset, which
129 may be useful to inform drought relief management strategies for the continent. The dataset covers the
130 period from 1981 to 2016 and it is comprehensively inter-compared with soil moisture, vegetation index and
131 coarse resolution SPEI datasets.

132 **2 Data and Methodology**

133 2.1 Data

134 2.1.1 CHIRPS

135 CHIRPS is a recently-developed high-resolution, daily, pentadal, dekadal, and monthly precipitation dataset
136 (Funk et al., 2015a). It was produced by blending a set of satellite-only precipitation values (CHIRP) with
137 additional monthly and pentadal station observations. The CHIRP is based on infrared cold cloud duration
138 (CCD) estimates calibrated with the Tropical Rainfall Measuring Mission Multi-satellite Precipitation
139 Analysis version 7 (TMPA 3B42 v7) and the Climate Hazards group Precipitation climatology (CHPclim)
140 The CHP_{clim} (Funk et al., 2015a; Funk et al., 2015e) is based on station data from the Food and Agriculture
141 Organization (FAO) and the Global Historical Climate Network (GHCN). Compared with other global
142 precipitation datasets such as Multi-Source Weighted-Ensemble Precipitation (MSWEP) (Beck et al., 2017)
143 and Global Precipitation Climatology Project (GPCP) (Adler et al., 2003), CHIRPS has several advantages:
144 a long period of record, high spatial resolution (5-km), low spatial biases and low temporal latency. It has
145 been widely validated and applied in various applications (e.g., Shukla et al., 2014; Maidment et al., 2015;
146 Duan et al., 2016; Zambrano-Bigiarini et al., 2017; Rivera et al., 2018). In particular, it was recently
147 validated over East Africa and Mozambique and demonstrated good performance compared to other
148 precipitation datasets (Toté et al., 2015; Dinku et al., 2018). Furthermore, CHIRPS was specifically designed
149 for drought monitoring over regions with deep convective precipitation, scarce observation networks and
150 complex topography (Funk et al., 2014). Several studies (e.g., Toté et al., 2015; Guo et al., 2017) have used
151 CHIRPS for drought monitoring. Its high spatial resolution makes it particularly suitable for local-scale
152 studies, such as sub-basin drought monitoring, especially in areas with complex topography. The detailed
153 description of the dataset was provided by Funk et al. (2015a). In this study, daily CHIRPS precipitation
154 from 1981 to 2016 was used.

155 2.2.2 GLEAM

156 GLEAM is designed to estimate land surface evaporation and root-zone soil moisture from remote sensing
157 observations and reanalysis data (Miralles et al., 2011; Martens et al., 2017). Specifically, the Priestley-
158 Taylor equation is used to calculate potential evaporation within GLEAM based on near surface temperature
159 and net radiation, while the root zone soil moisture is obtained from a multilayer water balance driven by

160 precipitation observations and updated with microwave soil moisture estimates (Martens et al., 2017). The
161 actual evaporation is estimated by constraining potential evaporation with a multiplicative evaporative stress
162 factor based on root-zone soil moisture and Vegetation Optical Depth (VOD) estimates. The GLEAM
163 version 3a (v3a) provides global daily potential and actual evaporation, evaporative stress conditions and
164 root zone soil moisture from 1980 to 2018 at spatial resolution of 0.25° (Martens et al., 2017) (see
165 www.gleam.eu). GLEAM datasets have already been comprehensively evaluated against FLUXNET
166 observations and used for multiple hydro-meteorological applications (Greve et al., 2014; Miralles et al.,
167 2014; Trambauer et al., 2014; Forzieri et al., 2017; Lian et al., 2018; Richard et al., 2018; Vicente-Serrano et
168 al., 2018; Zhan et al., 2019). In particular, two recent studies detected global drought conditions based on
169 GLEAM potential and actual evaporation data (Vicente-Serrano et al., 2018; Peng et al., 2019c). For this
170 study, the GLEAM potential evaporation and root zone soil moisture were used.

171 2.2.3 CRU-TS

172 The global gridded CRU-TS datasets provide most widely-used climate variables including precipitation,
173 potential evaporation, diurnal temperature range, maximum and minimum temperature, mean temperature,
174 frost day frequency, cloud cover and vapour pressure (Harris et al., 2014). The CRU TS datasets were
175 produced using angular-distance weighting (ADW) interpolation based on monthly meteorological
176 observations collected at ground-based stations across the world. The recently-released CRU TS version
177 4.0.1 covers the period 1901–2016 and provides monthly data at 50-km spatial resolution. The CRU TS
178 datasets have been widely used for various applications since their release (e.g., van der Schrier et al., 2013;
179 Chadwick et al., 2015; Delworth et al., 2015; Jägermeyr et al., 2016). The SPEIbase dataset was generated
180 from CRU TS datasets (Beguería et al., 2010). In this study, the CRU TS precipitation and potential
181 evaporation from 1981 to 2016 were used.

182 2.2.4 GIMMS NDVI

183 The Normalized Difference Vegetation Index (NDVI) can serve as a proxy of vegetation status and has been
184 widely applied to investigate the effects of drought on vegetation (e.g., Rojas et al., 2011; Vicente-Serrano et
185 al., 2013; Törnros and Menzel, 2014; Vicente-Serrano et al., 2018). The Global Inventory Monitoring and
186 Modeling System (GIMMS) NDVI was generated based on Advanced Very High Resolution Radiometer
187 (AVHRR) observations, and has accounted for various deleterious effects such as orbital drift, calibration
188 loss and volcanic eruptions (Beck et al., 2011; Pinzon and Tucker, 2014). For the current study, the latest
189 version of GIMMS NDVI (3g.v1) was used, which covers the time period from 1981 to 2015 at biweekly
190 temporal resolution and 8-km spatial resolution (Pinzon and Tucker, 2014).

191 2.3 Methods

192 2.3.1 SPEI calculation

193 The SPEI proposed by Vicente-Serrano et al. (2010) has been used for a wide variety of agricultural,
194 ecological and hydro-meteorological applications (e.g., Schwalm et al., 2017; Naumann et al., 2018; Jiang et
195 al., 2019). It accounts for the impacts of evaporation demand on droughts and inherits the simplicity and
196 multi-temporal characteristics of SPI. The procedure for SPEI calculation includes the estimation of a
197 climatic water balance (namely the difference between precipitation and potential evaporation), the
198 aggregation of the climatic water balance over various time-scales (e.g., 1, 3, 6, 12, 24, or more months), and
199 a fitting to a certain parameter distribution. As suggested by Beguería et al. (2014) and Vicente-Serrano and
200 Beguería (2016), the log-logistic probability distribution is best for SPEI calculation, from which the
201 probability distribution of the difference between precipitation and potential evaporation can be calculated as
202 suggested by Vicente-Serrano et al. (2010) and Beguería et al. (2014). The negative and positive SPEI values
203 respectively indicate dry and wet conditions. Table 1 summarizes the category of dry and wet conditions
204 based on SPEI values. In this study, the CHIRPS and GLEAM datasets were used for SPEI calculation at
205 high spatial resolution (5-km). For comparison, the SPEI at 50-km was also calculated based on CRU TS
206 datasets for the same 1981–2016 period. It should be noted that the SPEI over sparsely vegetated and barren
207 areas were masked out based on Moderate Resolution Imaging Spectroradiometer (MODIS) land cover

208 product (MCD12Q1) (Friedl et al., 2010), because SPEI is not reliable over these areas (Beguería et al., 2010;
209 Beguería et al., 2014; Zhao et al., 2017).

210 Table 1. Categories of dry and wet conditions indicated by SPEI values.

SPEI	Category
2 and above	Extremely wet
1.5 to 1.99	Very wet
1.0 to 1.49	Moderately wet
-0.99 to 0.99	Near Normal
-1.0 to -1.49	Moderately dry
-1.5 to -1.99	Severely dry
-2 and less	Extremely dry

211

212 2.3.2 Evaluation criteria

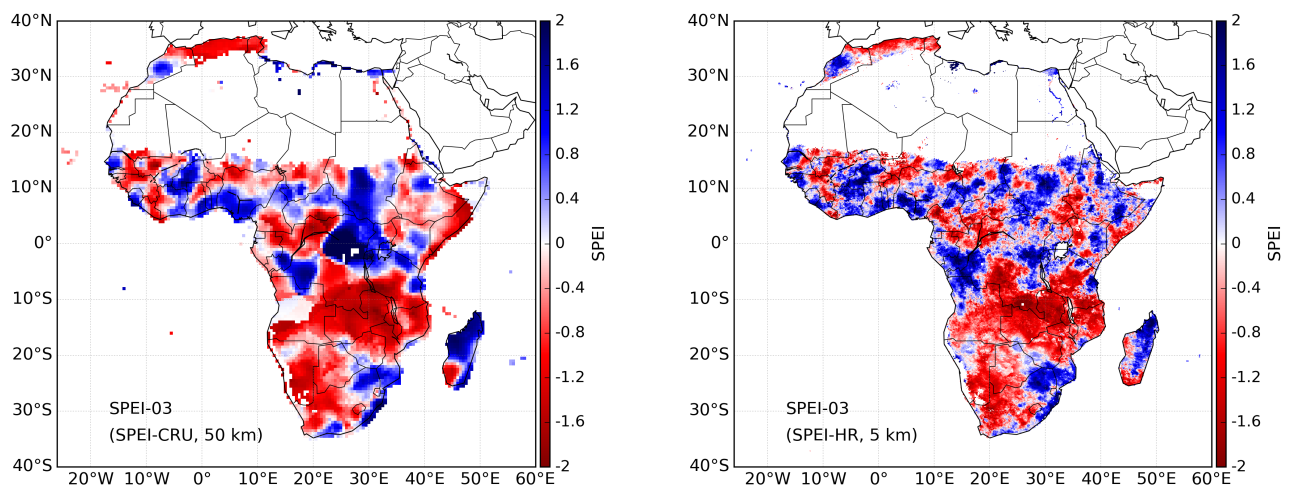
213 The SPEIbase dataset (Beguería et al., 2010) was calculated with CRU TS dataset, which has been evaluated
214 and applied by many studies (e.g., Chen et al., 2013; Vicente-Serrano et al., 2013; Isbell et al., 2015; Sun et
215 al., 2016a; Greenwood et al., 2017; Um et al., 2017). The newly-generated SPEI at high spatial resolution
216 based on CHIRPS and GLEAM (SPEI-HR) is compared temporally and spatially with the SPEI calculated
217 from CRU TS datasets. In addition, the NDVI can also serve as an indicator for drought and vegetation
218 health, and to assess the performance of drought indices (Vicente-Serrano et al., 2013; Aadhar and Mishra,
219 2017). Furthermore, root zone soil moisture is an ideal hydrological variable for agricultural (soil moisture)
220 drought monitoring. The recently-released root zone soil moisture (RSM) from GLEAM v3 provides a great
221 opportunity to evaluate whether soil moisture drought is well represented by SPEI. To facilitate direct
222 comparison between SPEI and NDVI as well as RSM, both NDVI and RSM are standardized by subtracting
223 their corresponding (1981–2016) mean and expressed the resulting anomalies as numbers of standard

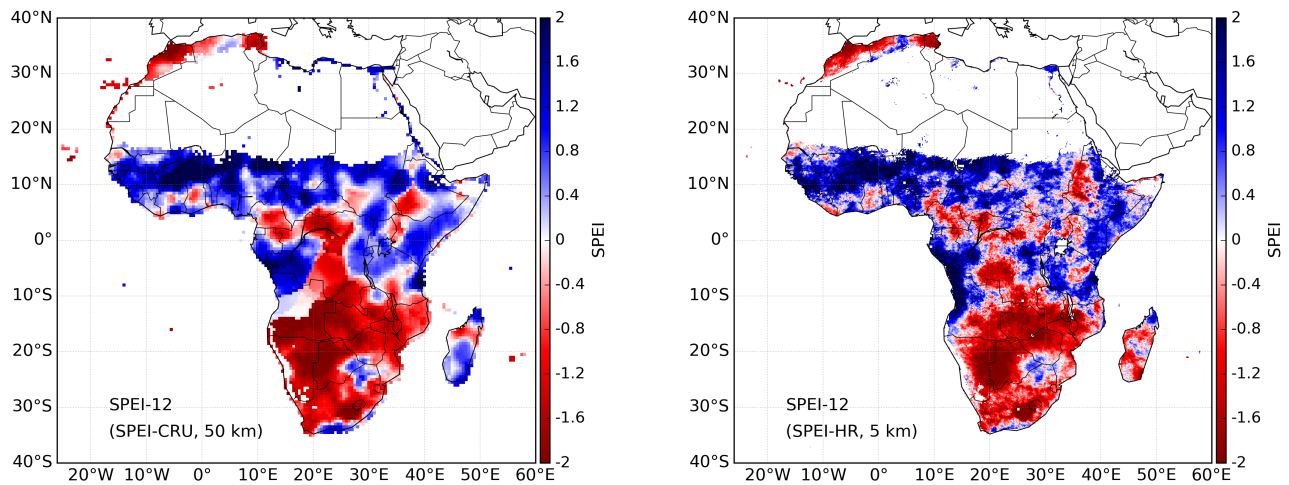
224 deviations. This standardization has been applied by many studies to evaluate drought indices (Anderson et
225 al., 2011; Mu et al., 2013; Zhao et al., 2017). The correlation between SPEI and the standardized NDVI and
226 RSM is quantified using Pearson's correlation coefficient (R). In addition, the high resolution SPEI from
227 GLEAM and CHIRPS is also resampled to the same grid size of SPEI from CRU TS in order to quantify
228 their correlation and disentangle whether the added value of the former arises from its increased accuracy or
229 higher resolution. In the following part, the high (5-km) resolution SPEI is referred to SPEI-HR, while the
230 coarse 50-km resolution SPEI is referred to SPEI-CRU.

231 **3 Results and discussion**

232 **3.1 Inter-comparison between high- and coarse-resolution SPEI**

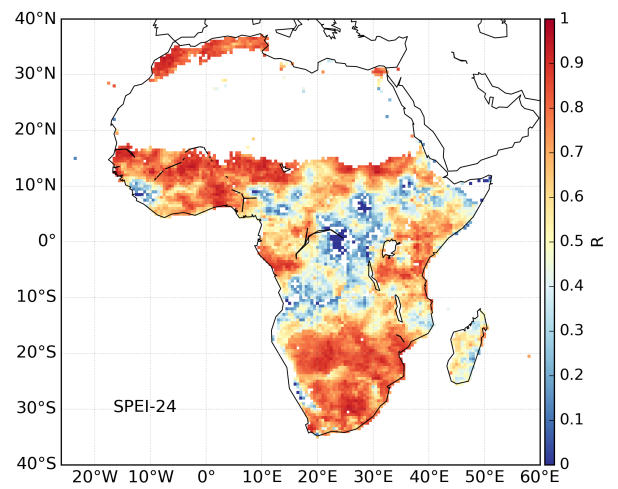
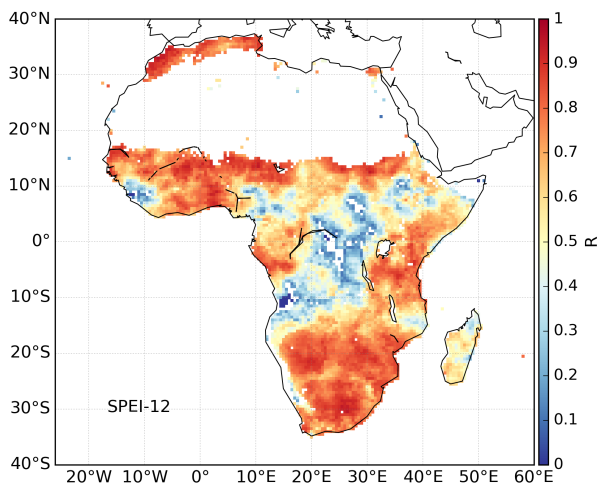
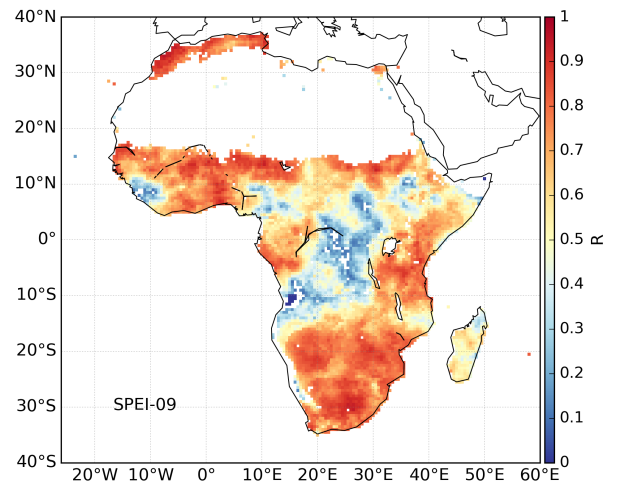
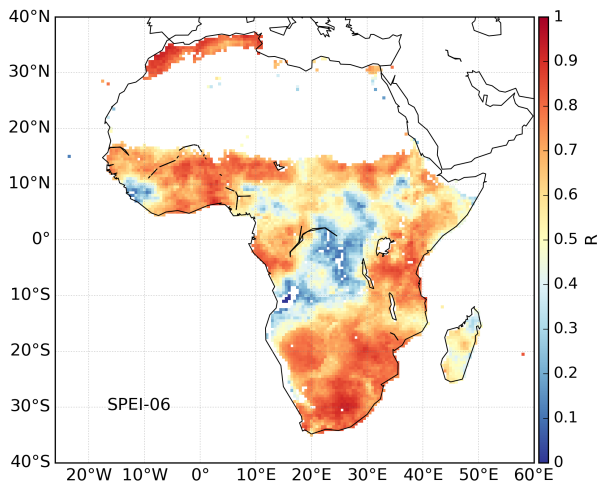
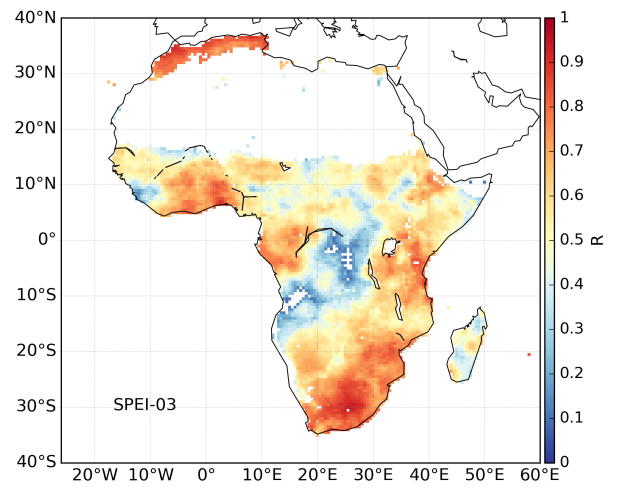
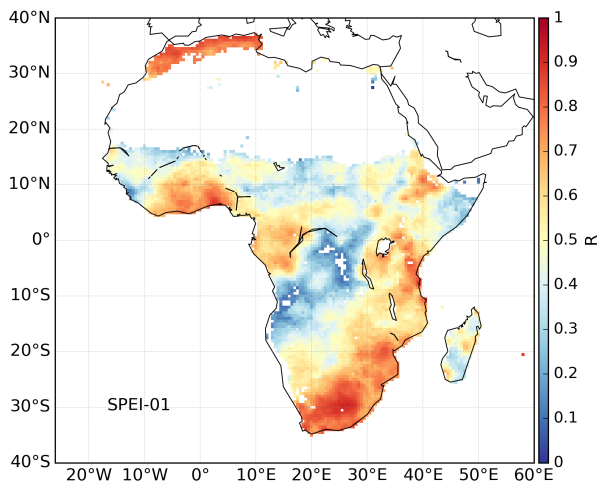
233 Figure 1 shows the spatial distribution of SPEI-HR and SPEI-CRU at different resolutions for an example
234 month (June 1995). Figure 1a,b show the 3-month SPEI and 12-month SPEI, respectively. It can be seen that
235 the high resolution and coarse resolution SPEI display quite similar dry and wet patterns over the whole of
236 Africa for both temporal scales. However, as expected, the SPEI-HR shows much more spatial detail that
237 reflects mesoscale geographic and climatic features, which highlights the advantages of this new dataset. The
238 differences in patterns between 3-month and 12-month SPEI indicate the different water deficits caused by
239 different aggregation time scales, which can further separate agricultural, hydrological, environmental, and
240 other droughts. For example, in June 1995 southern Africa showed persistent dry conditions over a
241 prolonged period, while western Africa only showed a short-term drought.

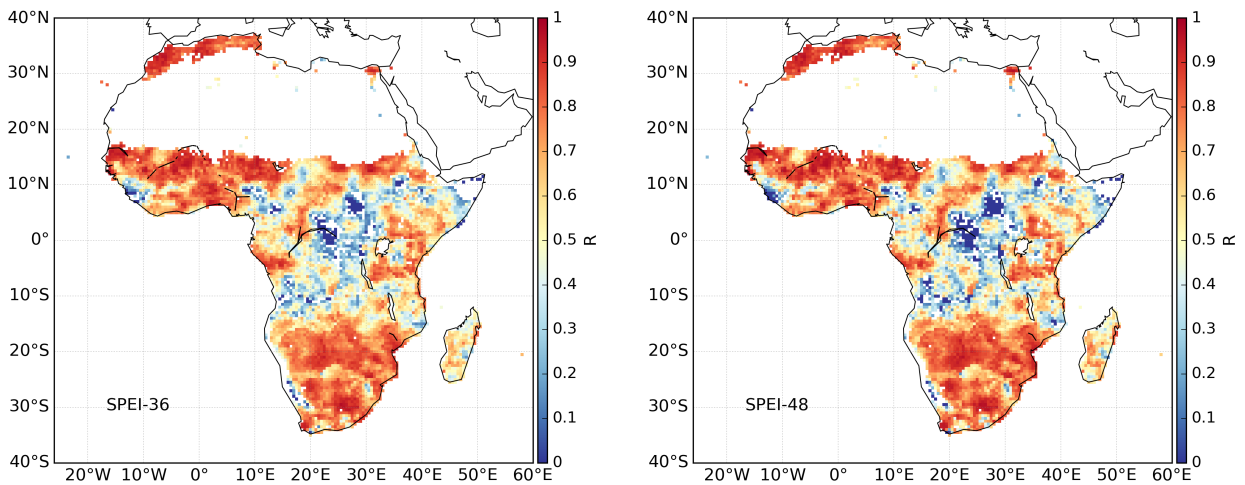




242
 243 Figure 1: Spatial patterns of 3-month and 12-month SPEI at high spatial resolution (5 km) and coarse spatial resolution (50 km) in
 244 June, 1995. The high spatial resolution SPEI (SPEI-HR) is based on CHIRPS precipitation and GLEAM potential evaporation,
 245 while the coarse spatial resolution SPEI (SPEI-CRU) is calculated from CRU TS datasets.
 246

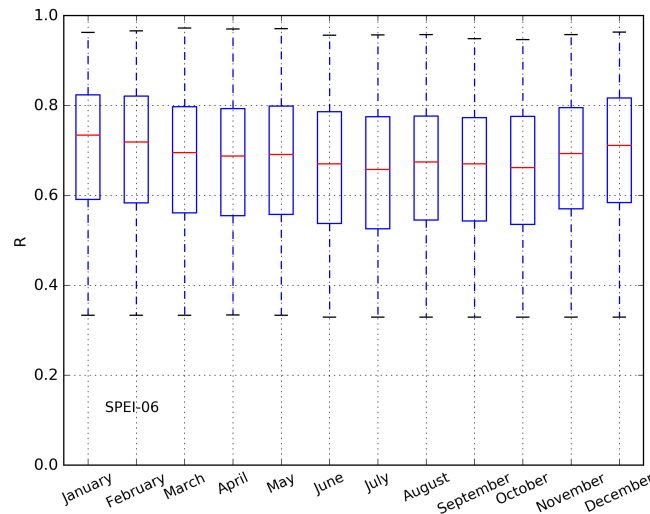
247 In order to quantify how different is SPEI-HR from SPEI-CRU, the correlation between them is calculated
 248 for each grid cell over the whole study period. Figure 2 shows the correlations for time-scales 1, 3, 6, 9, 12,
 249 24, 36, and 48 months. In general, the SPEI-HR and SPEI-CRU agree well in terms of temporal variability
 250 with high positive correlations over most of Africa for every time scale. However, relatively low correlations
 251 appear in central Africa, and they become lower as the SPEI time-scale increases. This region has very few
 252 station observations. It should be noted that the correlations shown here are statistically significant with p
 253 value less than 0.05. In addition, the average correlation between 6-month SPEI-CRU and SPEI-HR for
 254 each month of the year is summarized in Figure 3 using box plot. In general, positive correlations, with a
 255 median larger than 0.6 ($p < 0.05$), are found for every month. There are no substantial differences in
 256 correlations between different months. Figure A1 in Appendix shows additional box plots for SPEI at other
 257 time scales.





258
259
260

Figure 2: Correlation ($p < 0.05$) between SPEI-HR and SPEI-CRU, with the number indicating different months.



261
262
263
264
265

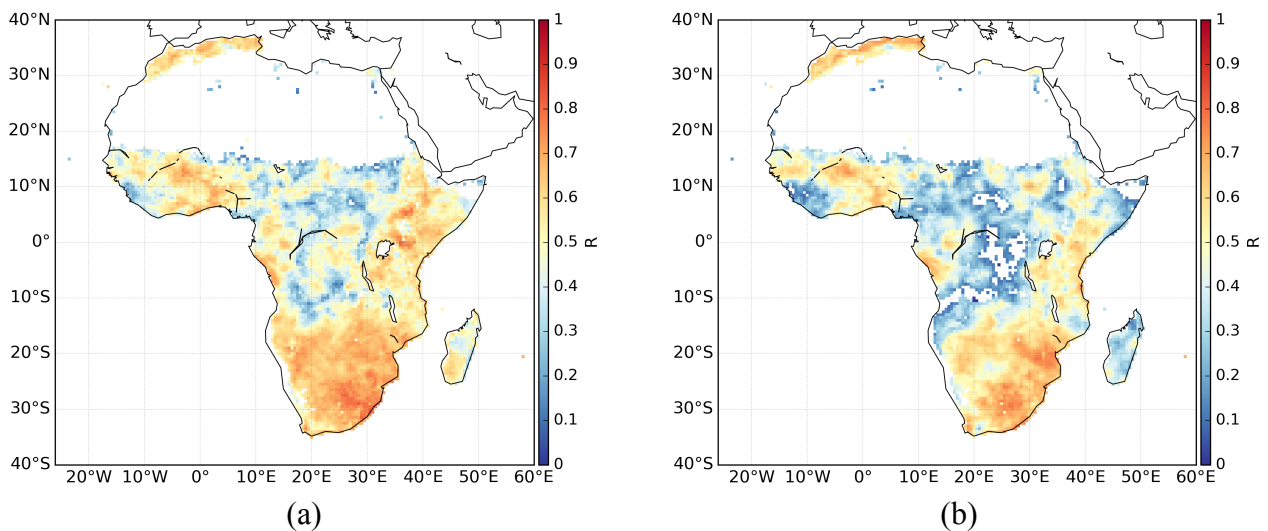
Figure 3: Box plot of the correlation ($p < 0.05$) between SPEI-HR and SPEI-CRU for each month of the entire record. The results here are based on 6-month SPEI and the red line in each box represents the median.

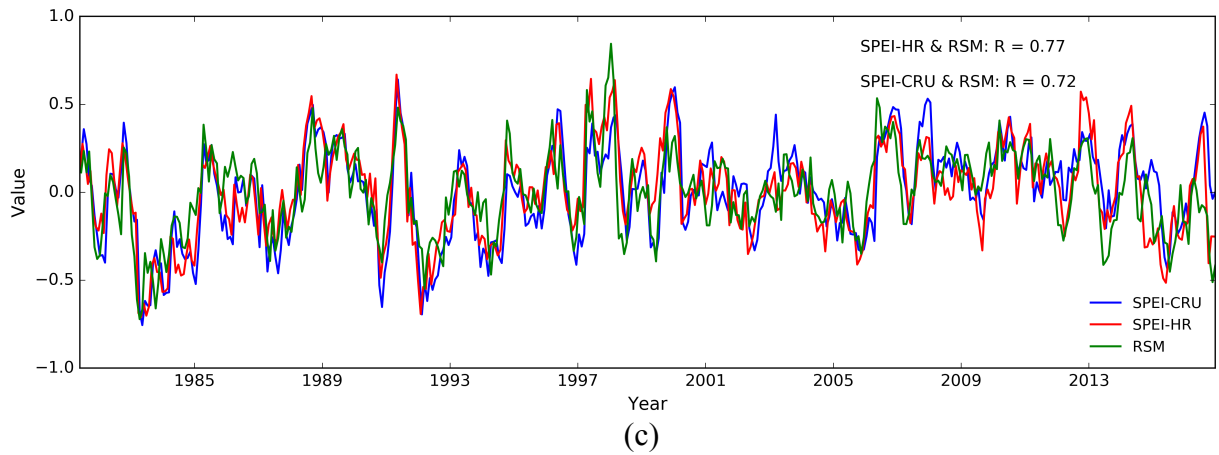
266 3.2 Comparison against root zone soil moisture and NDVI

267 To gain more insights into their significance and applicability, the SPEI datasets are compared with NDVI
 268 and RSM. Figure 4 shows the results of the spatial and temporal comparison between 6-month SPEI and
 269 RSM as indicated by Törnros and Menzel (2014). Figure 4a,b display the correlation ($p < 0.05$) of SPEI-HR
 270 and SPEI-CRU against RSM during the whole time period respectively. In general, both SPEI-HR and SPEI-
 271 CRU show strong correlations with RSM over the whole African continent. Compared to SPEI-CRU, the
 272 SPEI-HR shows higher correlations, particularly over central Africa. Since Section 3.1 shows that relatively

273 large discrepancy between SPEI-CRU and SPEI-HR exists over central Africa, the results presented here
274 suggest a potentially better performance of SPEI-HR compared with SPEI-CRU in this region.

275 The time series of SPEI and RSM, averaged over the entire study area, are shown in Figure 4c, together with
276 the corresponding correlations. It can be seen that both SPEI-HR and SPEI-CRU agree well with each other
277 and with the RSM dynamics. Consistent with the results from the spatial correlation analysis, the SPEI-HR
278 and SPEI-CRU show similar results when compared with RSM ($R = 0.77$ for SPEI-HR, $R = 0.72$ for SPEI-
279 CRU). Furthermore, the scatterplots between 6-month SPEI and RSM for the entire data record are shown in
280 Appendix Figure A2, where positive and significant correlations with RSM are found for both SPEI-HR ($R =$
281 0.51) and SPEI-CRU ($R = 0.42$). To explore the correlation between RSM and different time scales of SPEI,
282 Table 2 summarizes the correlation value calculated in the same way as Figure 4c. It can be seen that the
283 highest correlations against RSM are found at 3- and 6-month time scales. It should be noted that satellite
284 data-driven estimates of root zone soil moisture is more suitable for evaluating SPEI compared to satellite-
285 based top-layer soil moisture or reanalysis soil moisture data (Mo et al., 2011; Xu et al., 2018).





286 Figure 4: Spatial maps of correlation between SPEI and root zone soil moisture (RSM) for 6-month SPEI: (a) SPEI-HR and (b)
 287 SPEI-CRU. The time series of Africa area-mean RSM and SPEI are shown in (c), where R refers to the correlation coefficient.
 288 The correlations shown here are all significant at the 95% confidence level.
 289

290
 291 Table 2: The correlation ($p < 0.05$) between area-mean RSM and SPEI at different time scales.
 292

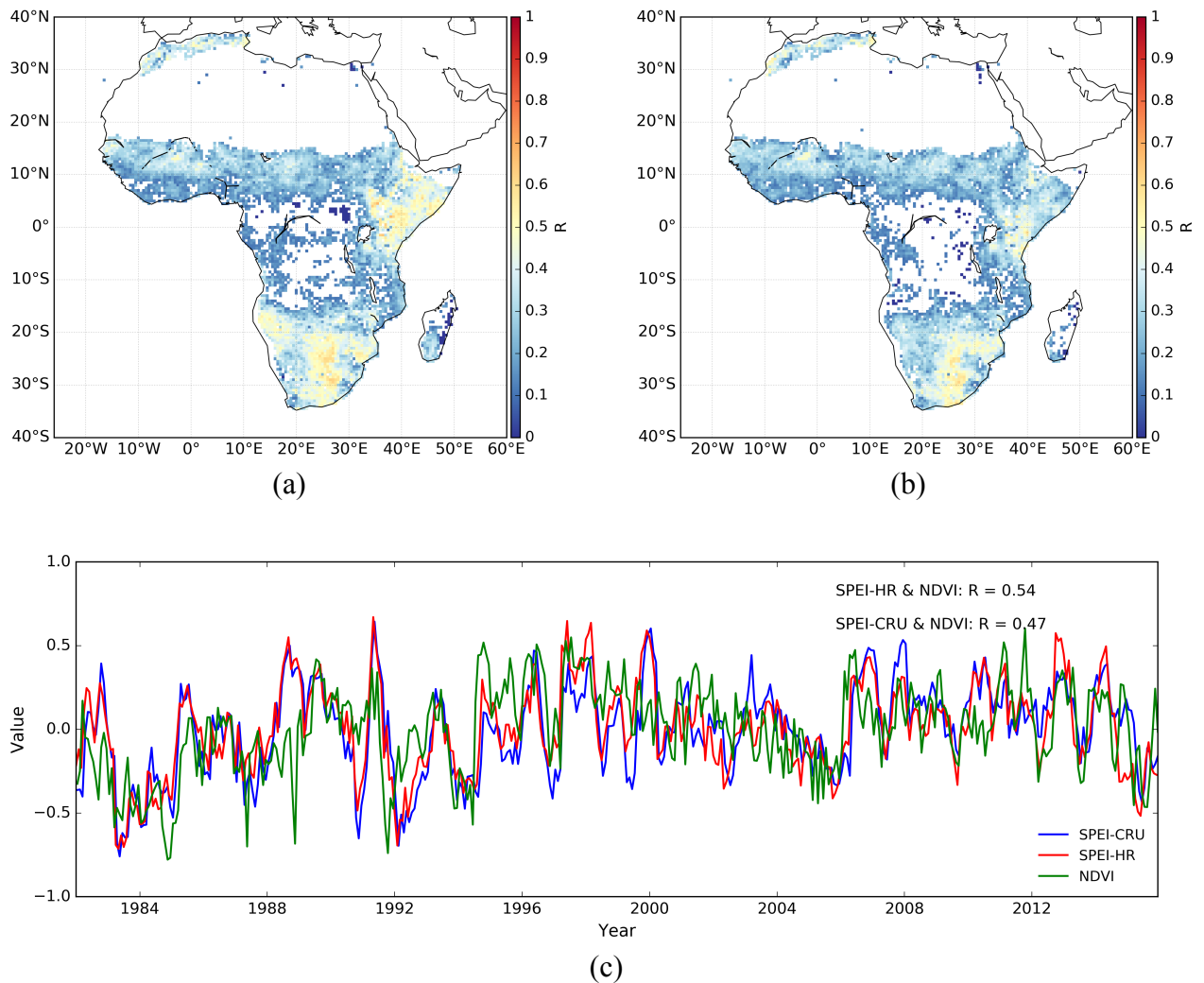
	SPEI-01	SPEI-03	SPEI-06	SPEI-09	SPEI-12	SPEI-24	SPEI-36	SPEI-48
R (SPEI-CRU)	0.52	0.74	0.72	0.64	0.56	0.41	0.26	0.16
R (SPEI-HR)	0.49	0.76	0.77	0.69	0.62	0.44	0.29	0.18

293

294 Similar to the above analysis between SPEI and RSM, the comparison of results between SPEI and NDVI
 295 are shown in Figure 5. First, Figures 5a,b present the spatial distribution of the correlations ($p < 0.05$) between
 296 SPEI-HR and NDVI and between SPEI-CRU and NDVI, respectively. While correlations are overall lower
 297 than for RSM, it can be seen that both SPEI datasets are positively correlated with NDVI over most of the
 298 continent. It is also clear that SPEI-HR shows higher correlations. The time series comparison between the
 299 area-mean SPEI and NDVI is shown in Figure 5c. Both SPEI-HR and SPEI-CRU show agreement with
 300 NDVI, with $R=0.54$ and $R=0.47$, respectively. In addition, the comparison between 6-month SPEI and
 301 NDVI for the entire data record was also calculated, with $R=0.24$ for SPEI-HR and $R=0.21$ for SPEI-CRU
 302 significant at 95% confidence level (Figure A3). While these correlations are admittedly low, overall results
 303 suggest that the SPEI has a positive relation with NDVI, which is also reported by previous studies (e.g.,
 304 Törnros and Menzel, 2014; Vicente-Serrano et al., 2018). The lower correlations against NDVI than against
 305 RSM are likely due to complex physiological processes associated to vegetation, and the fact that ecosystem
 306 state is driven by multiple variables other than water availability (Nemani et al., 2003). Furthermore, there

307 are also clearly documented lags between precipitation and NDVI, with NDVI time series typically peaking
 308 one or even two months after the period of maximum rainfall (Funk and Brown, 2006). Finally, Table 3
 309 summarizes the correlation between SPEI and NDVI at different time scales. Compared with the results
 310 presented in Table 2 for RSM, the correlation with NDVI shown in Table 3 is also generally lower, and the
 311 highest correlations appear between 9- and 24-month SPEI ($R > 0.5$).

312
 313
 314
 315



316
 317
 318 Figure 5: Spatial maps of the correlation between SPEI and NDVI for 6-month SPEI: (a) SPEI-HR and (b) SPEI-CRU. The time
 319 series of area-mean NDVI and SPEI are shown in (c), where R refers to the correlation coefficient. The correlations shown here
 320 are all significant at the 95% confidence level.
 321
 322

323 Table 3: The correlation ($p < 0.05$) between area-mean NDVI and SPEI at different time scales.
 324

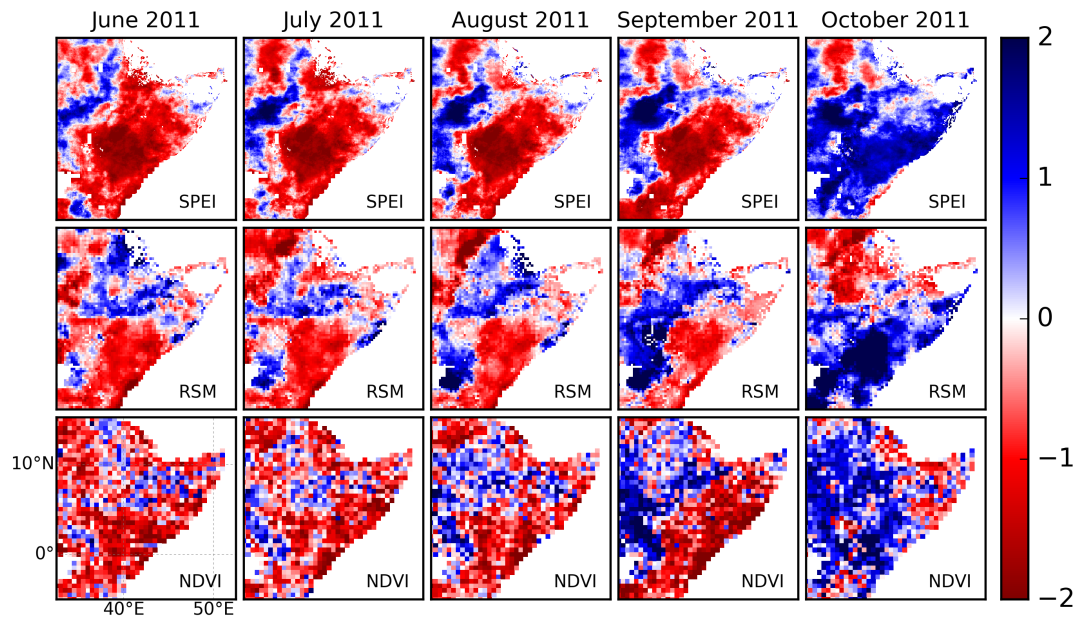
	SPEI-01	SPEI-03	SPEI-06	SPEI-09	SPEI-12	SPEI-24	SPEI-36	SPEI-48
R (SPEI-CRU)	0.23	0.42	0.47	0.48	0.47	0.50	0.34	0.20
R (SPEI-HR)	0.31	0.51	0.54	0.56	0.57	0.57	0.44	0.29

325

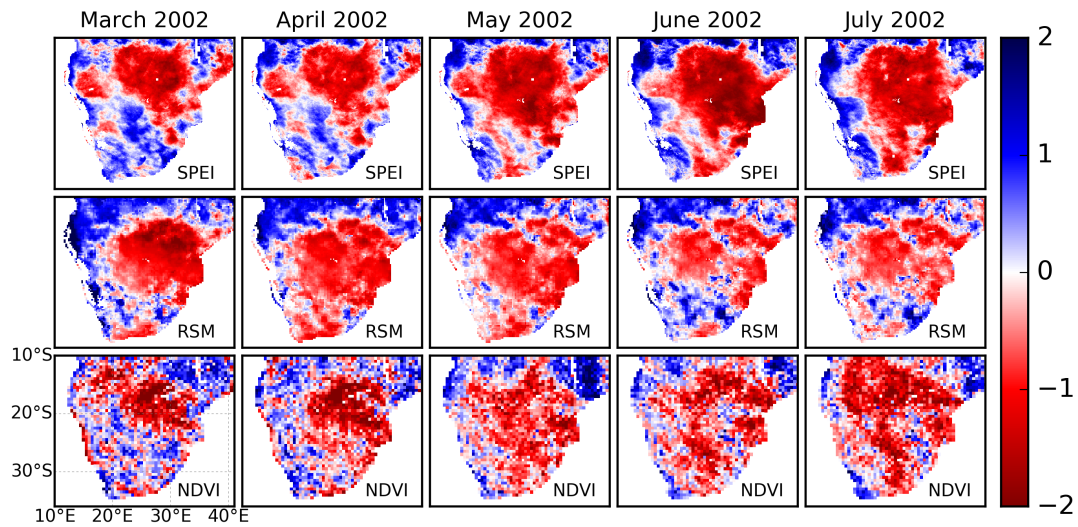
326 Altogether, the comparisons between SPEI and RSM and between SPEI and NDVI indirectly indicate the
327 validity of the generated SPEI datasets. Therefore, the generated high-resolution SPEI-HR from satellite
328 products has potential to improve upon the state of the art in drought assessment over Africa.

329 3.3 Patterns of SPEI, RSM and NDVI during specific drought events

330 Most of Africa has suffered severe droughts in past decades (Naumann et al., 2014; Blamey et al., 2018).
331 Among them, the 2011 East Africa drought (Anderson et al., 2012; AghaKouchak, 2015) and 2002 southern
332 Africa drought (Masih et al., 2014) were extremely severe and had devastating effects on the natural and
333 socioeconomic environment. Taking these two events as case studies, the spatial patterns of the newly-
334 developed high-resolution 6-month SPEI-HR are analyzed, together with the variability in NDVI and RSM.
335 Figure 6a,b show the evolution of 6-month SPEI, NDVI and RSM during the 2011 East Africa and the 2002
336 southern Africa drought, respectively. The 6-month periods end in the named month, with the 6-month June
337 2011 SPEI values based on data for January to June. In general, these three variables reflect the progressive
338 dry-out during the events. For example, strong, severe drought is revealed by the SPEI with values less than
339 -1.5, coinciding with a decline in NDVI and RSM, from June to September 2011 over East Africa; the
340 drought was offset in October. Similarly, dry and wet conditions variations during the 2002 southern Africa
341 drought were also captured by the three variables. Despite differences over space and time, results here
342 demonstrate that the generated SPEI-HR captures the main drought conditions that are reflected by negative
343 anomalies in NDVI and RSM, and can thus be used to study local drought related processes and societal
344 impacts in Africa.



(a)



(b)

345
346
347
348
349

Figure 6: Evolution of the spatial patterns of 6-month SPEI-HR, NDVI and root zone soil moisture (RSM) during the 2011 East Africa drought (a) and 2002 southern Africa drought (b), respectively.

350 4. Data availability

351 The high resolution SPEI dataset is publicly available from the Centre for Environmental Data Analysis
352 (CEDA) with link: <http://dx.doi.org/10.5285/bbdfd09a04304158b366777eba0d2aeb> (Peng et al., 2019a). It
353 covers the whole Africa at monthly temporal resolution and 5 km spatial resolution from 1981 to 2016, and
354 is provided with Geographic Lat/Lon projection and NetCDF format.

355

356 **5. Conclusion**

357 The study presents a newly-generated high-resolution SPEI dataset (SPEI-HR) over Africa. The dataset is
358 produced from satellite-based CHIRPS precipitation and GLEAM potential evaporation, and covers the
359 entire African continent over the time period from 1981 to 2016 with spatial resolution of 5-km. The
360 accumulated SPEI ranging from 1 to 48 months is provided to facilitate applications from meteorological to
361 hydrological droughts. The SPEI-HR was compared with widely used coarse-resolution SPEI data (SPEI-
362 CRU) and GIMMS NDVI as well as GLEAM root zone soil moisture to investigate its capability for drought
363 detection. In general, the SPEI-HR has good correlation with SPEI-CRU temporally and spatially. They both
364 agree well with NDVI and root zone soil moisture, although SPEI-HR displays higher correlations overall.
365 These results indicate the validity and advantage of the newly developed high resolution SPEI-HR dataset,
366 and its unprecedentedly high spatial resolution offers important advantages for drought monitoring and
367 assessment at district and river basin level in Africa.

368

369

370

371

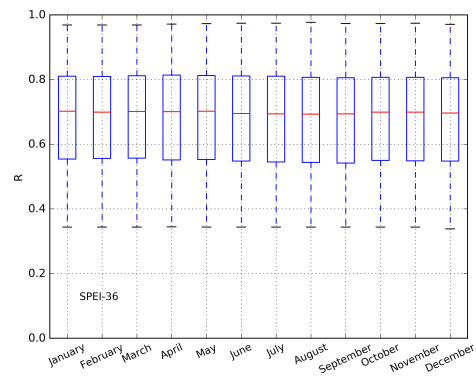
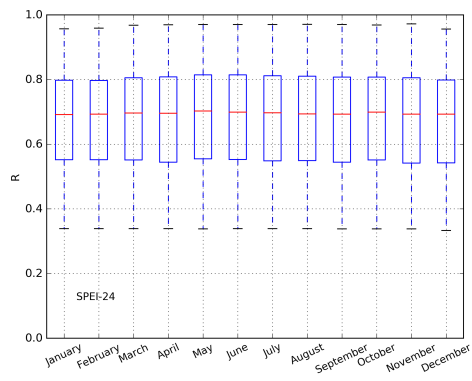
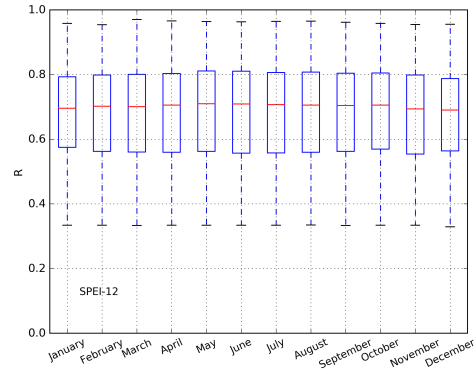
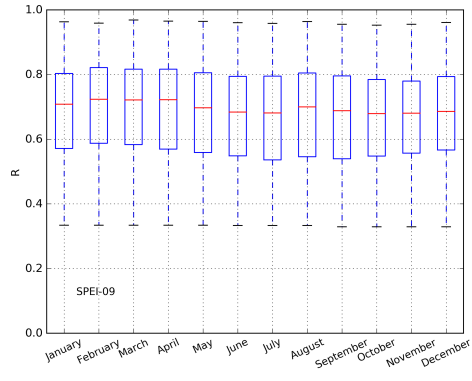
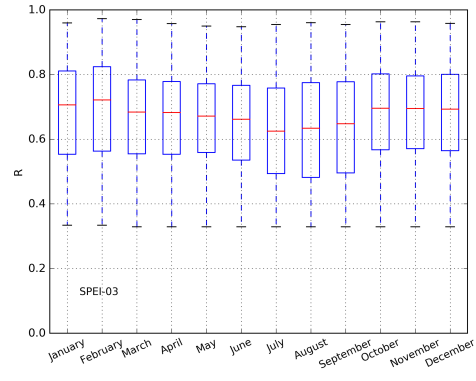
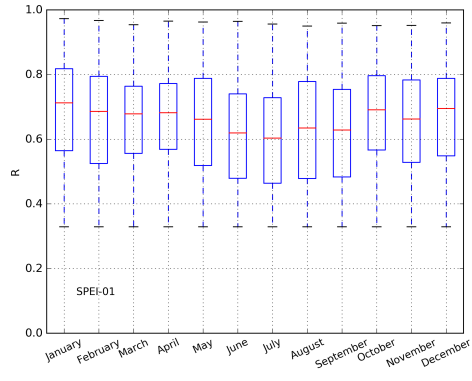
372

373

374

375

376



378

379

380

381

382

383

384

385

386

387

388

389

390

391

392

393

394

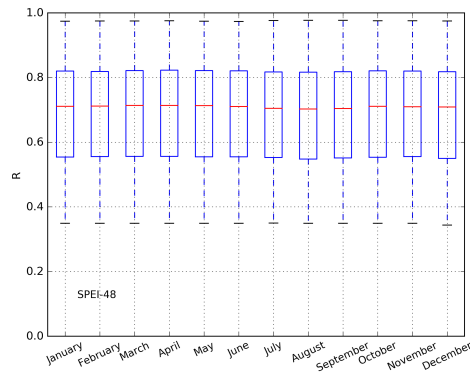
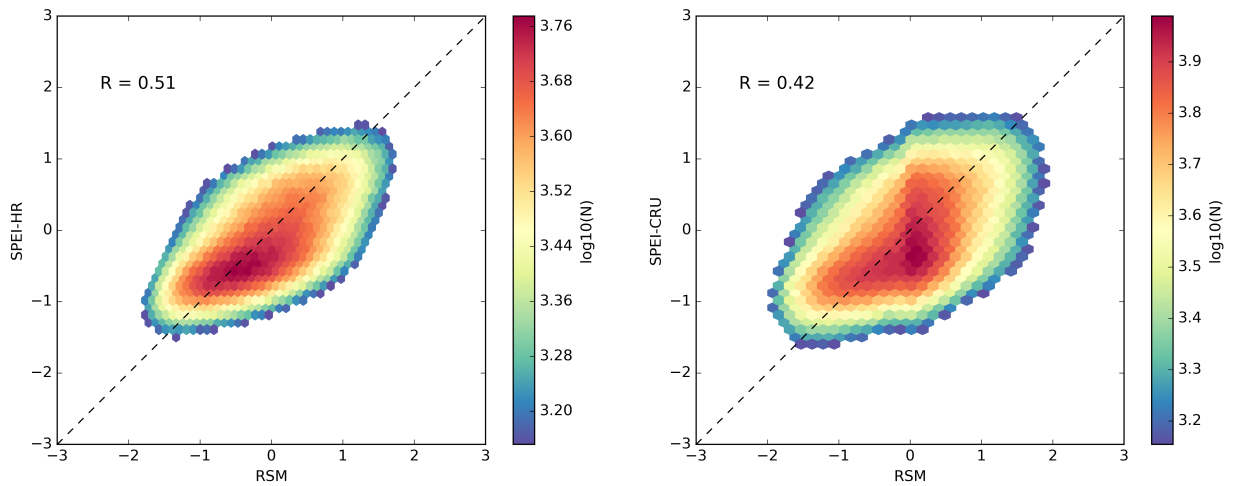


Figure A1: Box plots of the correlation ($p < 0.05$) between SPEI-HR and SPEI-CRU for each month and entire monthly record.



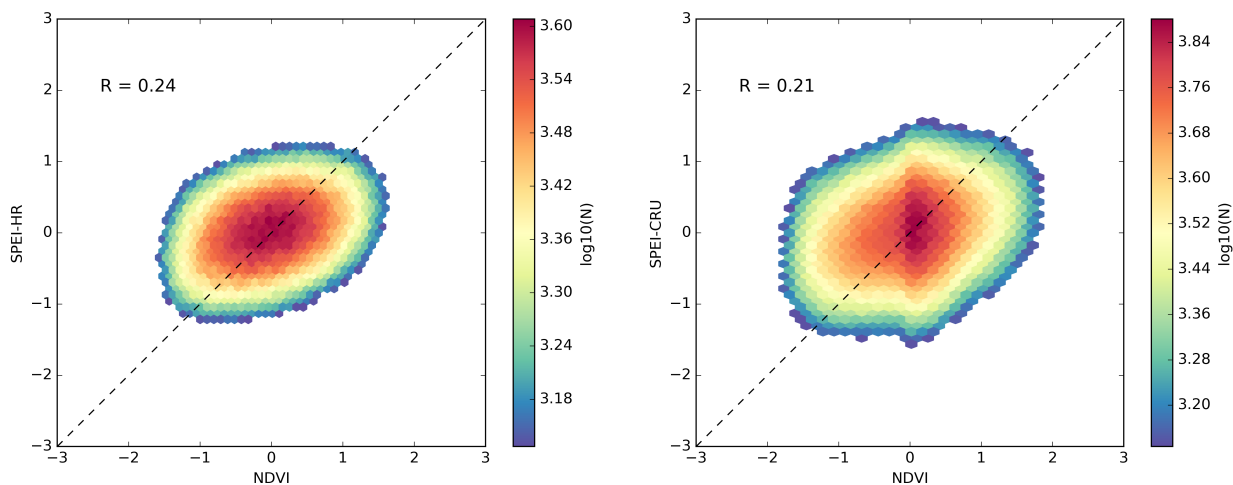
395

396

397

398

Figure A2: Scatterplots between 6-month SPEI and RSM for the entire data record. R is correlation coefficient with $p < 0.05$, and the colors denote the occurrence frequency of values.



399 Figure A3: Scatterplots between 6-month SPEI and NDVI for the entire data record. R is correlation coefficient with $p < 0.05$, and
400 the colors denote the occurrence frequency of values.
401

402 **Author contributions**

403 JP developed the processing algorithm, generated the dataset and drafted of the manuscript. DGM and CF
404 produced the GLEAM and CHIRPS data as input. SD, FH, ED and TL supported the generation of the
405 dataset and the analysis of the results. All authors contributed to the discussion, review and revision of this
406 manuscript.

407 **Competing interests**

408 The authors declare that they have no conflict of interest.

409 **Acknowledgments**

410 This work is supported by the UK Space Agency's International Partnership Programme (417000001429).
411 D.G.M. acknowledges funding from the European Research Council (ERC) under grant agreement 715254
412 (DRY-2-DRY). SD is also funded by the Natural Environment Research Council (NE/M020339/1). CF is
413 supported by the U.S. Geological Survey's Drivers of Drought program and NASA Harvest Program grant
414 Z60592017.

415

418 **References**

- 419 Aadhar, S. and Mishra, V.: High-resolution near real-time drought monitoring in South Asia, *Scientific data*, 4, 170145, 2017.
- 420 Adler, R. F., Huffman, G. J., Chang, A., Ferraro, R., Xie, P.-P., Janowiak, J., Rudolf, B., Schneider, U., Curtis, S., Bolvin, D.,
421 Gruber, A., Susskind, J., Arkin, P., and Nelkin, E.: The Version-2 Global Precipitation Climatology Project (GPCP) Monthly
422 Precipitation Analysis (1979–Present), *Journal of Hydrometeorology*, 4, 1147-1167, 2003.
- 423 AghaKouchak, A.: A multivariate approach for persistence-based drought prediction: Application to the 2010–2011 East Africa
424 drought, *Journal of Hydrology*, 526, 127-135, 2015.
- 425 AghaKouchak, A., Farahmand, A., Melton, F. S., Teixeira, J., Anderson, M. C., Wardlow, B. D., and Hain, C. R.: Remote sensing
426 of drought: Progress, challenges and opportunities, *Reviews of Geophysics*, 53, 452-480, 2015.
- 427 Anderson, M. C., Hain, C., Wardlow, B., Pimstein, A., Mecikalski, J. R., and Kustas, W. P.: Evaluation of drought indices based
428 on thermal remote sensing of evapotranspiration over the continental United States, *Journal of Climate*, 24, 2025-2044, 2011.
- 429 Anderson, W. B., Zaitchik, B. F., Hain, C. R., Anderson, M. C., Yilmaz, M. T., Mecikalski, J., and Schultz, L.: Towards an
430 integrated soil moisture drought monitor for East Africa, *Hydrol. Earth Syst. Sci.*, 16, 2893-2913, 2012.
- 431 Anghileri, D., Li, C., Agaba, G., Kandel, M., Dash, J., Reeves, J., Lewis, L., Hill, C., and Sheffield, J.: Co-production and
432 interdisciplinary research in the BRECCIA project: bringing together different expertise and actors for addressing water and food
433 security challenges in sub-Saharan Africa, *Geophysical Research Abstracts*2019, EGU2019-14992.
- 434 Arpe, K., Leroy, S., Lahijani, H., and Khan, V.: Impact of the European Russia drought in 2010 on the Caspian Sea level,
435 *Hydrology and earth system science*, 16, 19-27, 2012.
- 436 Awange, J. L., Khandu, Schumacher, M., Forootan, E., and Heck, B.: Exploring hydro-meteorological drought patterns over the
437 Greater Horn of Africa (1979–2014) using remote sensing and reanalysis products, *Advances in Water Resources*, 94, 45-59,
438 2016.
- 439 Bachmair, S., Stahl, K., Collins, K., Hannaford, J., Acreman, M., Svoboda, M., Knutson, C., Smith, K. H., Wall, N., and Fuchs,
440 B.: Drought indicators revisited: the need for a wider consideration of environment and society, *Wiley Interdisciplinary Reviews:*
441 *Water*, 3, 516-536, 2016.
- 442 Bachmair, S., Tanguy, M., Hannaford, J., and Stahl, K.: How well do meteorological indicators represent agricultural and forest
443 drought across Europe?, *Environmental Research Letters*, 13, 034042, 2018.
- 444 Baudoin, M.-A., Vogel, C., Nortje, K., and Naik, M.: Living with drought in South Africa: lessons learnt from the recent El Niño
445 drought period, *International Journal of Disaster Risk Reduction*, 23, 128-137, 2017.
- 446 Beck, H. E., McVicar, T. R., van Dijk, A. I., Schellekens, J., de Jeu, R. A., and Bruijnzeel, L. A.: Global evaluation of four
447 AVHRR–NDVI data sets: Intercomparison and assessment against Landsat imagery, *Remote Sensing of Environment*, 115, 2547-
448 2563, 2011.
- 449 Beck, H. E., Van Dijk, A. I., Levizzani, V., Schellekens, J., Gonzalez Miralles, D., Martens, B., and De Roo, A.: MSWEP: 3-
450 hourly 0.25 global gridded precipitation (1979-2015) by merging gauge, satellite, and reanalysis data, *Hydrology and Earth*
451 *System Sciences*, 21, 589-615, 2017.
- 452 Becker, A., Finger, P., Meyer-Christoffer, A., Rudolf, B., Schamm, K., Schneider, U., and Ziese, M.: A description of the global
453 land-surface precipitation data products of the Global Precipitation Climatology Centre with sample applications including
454 centennial (trend) analysis from 1901–present, *Earth System Science Data*, 5, 71-99, 2013.
- 455 Beguería, S., Vicente-Serrano, S. M., and Angulo-Martínez, M.: A multiscalar global drought dataset: the SPEIbase: a new
456 gridded product for the analysis of drought variability and impacts, *Bulletin of the American Meteorological Society*, 91, 1351-
457 1356, 2010.
- 458 Beguería, S., Vicente-Serrano, S. M., Reig, F., and Latorre, B.: Standardized precipitation evapotranspiration index (SPEI)
459 revisited: parameter fitting, evapotranspiration models, tools, datasets and drought monitoring, *International Journal of*
460 *Climatology*, 34, 3001-3023, 2014.
- 461 Blamey, R. C., Kolusu, S. R., Mahlalela, P., Todd, M. C., and Reason, C. J. C.: The role of regional circulation features in
462 regulating El Niño climate impacts over southern Africa: A comparison of the 2015/2016 drought with previous events,
463 *International Journal of Climatology*, 0, 2018.
- 464 Chadwick, R., Good, P., Martin, G., and Rowell, D. P.: Large rainfall changes consistently projected over substantial areas of
465 tropical land, *Nature Climate Change*, 6, 177, 2015.
- 466 Chen, T., Werf, G. R., Jeu, R. A. M., Wang, G., and Dolman, A. J.: A global analysis of the impact of drought on net primary
467 productivity, *Hydrol. Earth Syst. Sci.*, 17, 3885-3894, 2013.
- 468 Crausbay, S. D., Ramirez, A. R., Carter, S. L., Cross, M. S., Hall, K. R., Bathke, D. J., Betancourt, J. L., Colt, S., Cravens, A. E.,
469 and Dalton, M. S.: Defining ecological drought for the twenty-first century, *Bulletin of the American Meteorological Society*, 98,
470 2543-2550, 2017.

471 Dadson, S. J., Lopez, H. P., Peng, J., and Vora, S.: Hydroclimatic Extremes and Climate Change, *Water Science, Policy, and*
472 *Management: A Global Challenge*, doi: 10.1002/9781119520627.ch2, 2019. 11-28, 2019.

473 Delworth, T. L., Zeng, F., Rosati, A., Vecchi, G. A., and Wittenberg, A. T.: A Link between the Hiatus in Global Warming and
474 North American Drought, *Journal of Climate*, 28, 3834-3845, 2015.

475 Deo, R. C., Byun, H.-R., Adamowski, J. F., and Begum, K.: Application of effective drought index for quantification of
476 meteorological drought events: a case study in Australia, *Theoretical and Applied Climatology*, 128, 359-379, 2017.

477 Ding, Y., Hayes, M. J., and Widhalm, M.: Measuring economic impacts of drought: a review and discussion, *Disaster Prevention*
478 *and Management: An International Journal*, 20, 434-446, 2011.

479 Dinku, T., Funk, C., Peterson, P., Maidment, R., Tadesse, T., Gadain, H., and Ceccato, P.: Validation of the CHIRPS satellite
480 rainfall estimates over eastern Africa, *Quarterly Journal of the Royal Meteorological Society*, 0, 2018.

481 Duan, Z., Liu, J., Tuo, Y., Chiogna, G., and Disse, M.: Evaluation of eight high spatial resolution gridded precipitation products in
482 Adige Basin (Italy) at multiple temporal and spatial scales, *Science of The Total Environment*, 573, 1536-1553, 2016.

483 Fan, Y. and Van den Dool, H.: A global monthly land surface air temperature analysis for 1948–present, *Journal of Geophysical*
484 *Research: Atmospheres*, 113, 2008.

485 Fisher, J. B., Melton, F., Middleton, E., Hain, C., Anderson, M., Allen, R., McCabe, M. F., Hook, S., Baldocchi, D., and
486 Townsend, P. A.: The future of evapotranspiration: Global requirements for ecosystem functioning, carbon and climate feedbacks,
487 agricultural management, and water resources, *Water Resources Research*, 53, 2618-2626, 2017.

488 Forzieri, G., Alkama, R., Miralles, D. G., and Cescatti, A.: Satellites reveal contrasting responses of regional climate to the
489 widespread greening of Earth, *Science*, 356, 1180-1184, 2017.

490 Friedl, M. A., Sulla-Menashe, D., Tan, B., Schneider, A., Ramankutty, N., Sibley, A., and Huang, X.: MODIS Collection 5 global
491 land cover: Algorithm refinements and characterization of new datasets, *Remote sensing of Environment*, 114, 168-182, 2010.

492 Funk, C., Harrison, L., Shukla, S., Pomposi, C., Galu, G., Korecha, D., Husak, G., Magadzire, T., Davenport, F., and Hillbruner,
493 C.: Examining the role of unusually warm Indo-Pacific sea-surface temperatures in recent African droughts, *Quarterly Journal of*
494 *the Royal Meteorological Society*, 144, 360-383, 2018.

495 Funk, C., Peterson, P., Landsfeld, M., Pedreros, D., Verdin, J., Shukla, S., Husak, G., Rowland, J., Harrison, L., Hoell, A., and
496 Michaelsen, J.: The climate hazards infrared precipitation with stations—a new environmental record for monitoring extremes,
497 *Scientific Data*, 2, 150066, 2015a.

498 Funk, C., Verdin, A., Michaelsen, J., Peterson, P., Pedreros, D., and Husak, G.: A global satellite-assisted precipitation
499 climatology, *Earth Syst. Sci. Data*, 7, 275-287, 2015e.

500 Funk, C. C. and Brown, M. E.: Intra-seasonal NDVI change projections in semi-arid Africa, *Remote Sensing of Environment*, 101,
501 249-256, 2006.

502 Funk, C. C., Peterson, P. J., Landsfeld, M. F., Pedreros, D. H., Verdin, J. P., Rowland, J. D., Romero, B. E., Husak, G. J.,
503 Michaelsen, J. C., and Verdin, A. P.: A quasi-global precipitation time series for drought monitoring, *US Geological Survey Data*
504 *Series*, 832, 2014.

505 García-Herrera, R., Díaz, J., Trigo, R. M., Luterbacher, J., and Fischer, E. M.: A review of the European summer heat wave of
506 2003, *Critical Reviews in Environmental Science and Technology*, 40, 267-306, 2010.

507 Gebremeskel, G., Tang, Q., Sun, S., Huang, Z., Zhang, X., and Liu, X.: Droughts in East Africa: Causes, impacts and resilience,
508 *Earth-Science Reviews*, 2019. 2019.

509 Greenwood, S., Ruiz-Benito, P., Martínez-Vilalta, J., Lloret, F., Kitzberger, T., Allen, C. D., Fensham, R., Laughlin, D. C., Kattge,
510 J., and Bönisch, G.: Tree mortality across biomes is promoted by drought intensity, lower wood density and higher specific leaf
511 area, *Ecology Letters*, 20, 539-553, 2017.

512 Greve, P., Orłowsky, B., Mueller, B., Sheffield, J., Reichstein, M., and Seneviratne, S. I.: Global assessment of trends in wetting
513 and drying over land, *Nature geoscience*, 7, 716, 2014.

514 Griffin, D. and Anchukaitis, K. J.: How unusual is the 2012–2014 California drought?, *Geophysical Research Letters*, 41, 9017-
515 9023, 2014.

516 Guo, H., Bao, A., Liu, T., Ndayisaba, F., He, D., Kurban, A., and De Maeyer, P.: Meteorological drought analysis in the Lower
517 Mekong Basin using satellite-based long-term CHIRPS product, *Sustainability*, 9, 901, 2017.

518 Harris, I., Jones, P. D., Osborn, T. J., and Lister, D. H.: Updated high-resolution grids of monthly climatic observations – the CRU
519 TS3.10 Dataset, *International Journal of Climatology*, 34, 623-642, 2014.

520 Heim Jr, R. R.: A review of twentieth-century drought indices used in the United States, *Bulletin of the American Meteorological*
521 *Society*, 83, 1149-1165, 2002.

522 Isbell, F., Craven, D., Connolly, J., Loreau, M., Schmid, B., Beierkuhnlein, C., Bezemer, T. M., Bonin, C., Bruelheide, H., de
523 Luca, E., Ebeling, A., Griffin, J. N., Guo, Q., Hautier, Y., Hector, A., Jentsch, A., Kreyling, J., Lanta, V., Manning, P., Meyer, S.
524 T., Mori, A. S., Naeem, S., Niklaus, P. A., Polley, H. W., Reich, P. B., Roscher, C., Seabloom, E. W., Smith, M. D., Thakur, M.
525 P., Tilman, D., Tracy, B. F., van der Putten, W. H., van Ruijven, J., Weigelt, A., Weisser, W. W., Wilsey, B., and Eisenhauer, N.:
526 Biodiversity increases the resistance of ecosystem productivity to climate extremes, *Nature*, 526, 574, 2015.

527 Jägermeyr, J., Gerten, D., Schaphoff, S., Heinke, J., Lucht, W., and Rockström, J.: Integrated crop water management might
528 sustainably halve the global food gap, *Environmental Research Letters*, 11, 025002, 2016.

529 Jiang, P., Liu, H., Piao, S., Ciais, P., Wu, X., Yin, Y., and Wang, H.: Enhanced growth after extreme wetness compensates for
530 post-drought carbon loss in dry forests, *Nature Communications*, 10, 195, 2019.

531 Keyantash, J. and Dracup, J. A.: The quantification of drought: an evaluation of drought indices, *Bulletin of the American*
532 *Meteorological Society*, 83, 1167-1180, 2002.

533 Kumar, R., Musuza, J. L., Loon, A. F. V., Teuling, A. J., Barthel, R., Ten Broek, J., Mai, J., Samaniego, L., and Attinger, S.:
534 Multiscale evaluation of the Standardized Precipitation Index as a groundwater drought indicator, *Hydrology and Earth System*
535 *Sciences*, 20, 1117-1131, 2016.

536 Lian, X., Piao, S., Huntingford, C., Li, Y., Zeng, Z., Wang, X., Ciais, P., McVicar, T. R., Peng, S., Ottlé, C., Yang, H., Yang, Y.,
537 Zhang, Y., and Wang, T.: Partitioning global land evapotranspiration using CMIP5 models constrained by observations, *Nature*
538 *Climate Change*, 8, 640-646, 2018.

539 Lloyd-Hughes, B.: The impracticality of a universal drought definition, *Theoretical and Applied Climatology*, 117, 607-611, 2014.

540 Maidment, R. I., Allan, R. P., and Black, E.: Recent observed and simulated changes in precipitation over Africa, *Geophysical*
541 *Research Letters*, 42, 8155-8164, 2015.

542 Mann, M. E. and Gleick, P. H.: Climate change and California drought in the 21st century, *Proceedings of the National Academy*
543 *of Sciences*, 112, 3858-3859, 2015.

544 Martens, B., Miralles, D. G., Lievens, H., van der Schalie, R., de Jeu, R. A., Fernández-Prieto, D., Beck, H. E., Dorigo, W. A., and
545 Verhoest, N. E.: GLEAM v3: satellite-based land evaporation and root-zone soil moisture, *Geoscientific Model Development*, 10,
546 1903, 2017.

547 Marvel, K., Cook, B. I., Bonfils, C. J., Durack, P. J., Smerdon, J. E., and Williams, A. P.: Twentieth-century hydroclimate changes
548 consistent with human influence, *Nature*, 569, 59, 2019.

549 Masih, I., Maskey, S., Mussá, F., and Trambauer, P.: A review of droughts on the African continent: a geospatial and long-term
550 perspective, *Hydrology and Earth System Sciences*, 18, 3635-3649, 2014.

551 McKee, T. B., Doesken, N. J., and Kleist, J.: The relationship of drought frequency and duration to time scales, 1993, 179-183.

552 Miralles, D. G., Holmes, T. R. H., De Jeu, R. A. M., Gash, J. H., Meesters, A. G. C. A., and Dolman, A. J.: Global land-surface
553 evaporation estimated from satellite-based observations, *Hydrol. Earth Syst. Sci.*, 15, 453-469, 2011.

554 Miralles, D. G., Van Den Berg, M. J., Gash, J. H., Parinussa, R. M., De Jeu, R. A., Beck, H. E., Holmes, T. R., Jiménez, C.,
555 Verhoest, N. E., and Dorigo, W. A.: El Niño–La Niña cycle and recent trends in continental evaporation, *Nature Climate Change*,
556 4, 122, 2014.

557 Mishra, A. K. and Singh, V. P.: A review of drought concepts, *Journal of hydrology*, 391, 202-216, 2010.

558 Mo, K. C., Long, L. N., Xia, Y., Yang, S. K., Schemm, J. E., and Ek, M.: Drought Indices Based on the Climate Forecast System
559 Reanalysis and Ensemble NLDAS, *Journal of Hydrometeorology*, 12, 181-205, 2011.

560 Mu, Q., Zhao, M., Kimball, J. S., McDowell, N. G., and Running, S. W.: A remotely sensed global terrestrial drought severity
561 index, *Bulletin of the American Meteorological Society*, 94, 83-98, 2013.

562 Mukherjee, S., Mishra, A., and Trenberth, K. E.: Climate change and drought: a perspective on drought indices, *Current Climate*
563 *Change Reports*, 4, 145-163, 2018.

564 Muller, M.: Cape Town's drought: don't blame climate change. Nature Publishing Group, 2018.

565 Naumann, G., Alfieri, L., Wyser, K., Mentaschi, L., Betts, R. A., Carrao, H., Spinoni, J., Vogt, J., and Feyen, L.: Global Changes
566 in Drought Conditions Under Different Levels of Warming, *Geophysical Research Letters*, 45, 3285-3296, 2018.

567 Naumann, G., Dutra, E., Barbosa, P., Pappenberger, F., Wetterhall, F., and Vogt, J.: Comparison of drought indicators derived
568 from multiple data sets over Africa, *Hydrology and Earth System Sciences*, 18, 1625-1640, 2014.

569 Nemani, R. R., Keeling, C. D., Hashimoto, H., Jolly, W. M., Piper, S. C., Tucker, C. J., Myneni, R. B., and Running, S. W.:
570 Climate-Driven Increases in Global Terrestrial Net Primary Production from 1982 to 1999, *Science*, 300, 1560-1563, 2003.

571 Nicholson, S. E.: A detailed look at the recent drought situation in the Greater Horn of Africa, *Journal of Arid Environments*, 103,
572 71-79, 2014.

573 Nicholson, S. E.: The ITCZ and the seasonal cycle over equatorial Africa, *Bulletin of the American Meteorological Society*, 99,
574 337-348, 2018.

575 Panu, U. and Sharma, T.: Challenges in drought research: some perspectives and future directions, *Hydrological Sciences Journal*,
576 47, S19-S30, 2002.

577 Peña-Gallardo, M., Vicente-Serrano, S., Camarero, J., Gazol, A., Sánchez-Salguero, R., Domínguez-Castro, F., El Kenawy, A.,
578 Beguería-Portugés, S., Gutiérrez, E., and de Luis, M.: Drought Sensitiveness on Forest Growth in Peninsular Spain and the
579 Balearic Islands, *Forests*, 9, 524, 2018a.

580 Peña-Gallardo, M., Vicente-Serrano, S. M., Domínguez-Castro, F., Quiring, S., Svoboda, M., Beguería, S., and Hannaford, J.:
581 Effectiveness of drought indices in identifying impacts on major crops across the USA, *Climate Research*, 75, 221-240, 2018b.

582 Peng, J., Dadson, S., Hirpa, F., Dyer, E., Lees, T., Miralles, D. G., Vicente-Serrano, S. M. V.-S., and Funk, C.: High resolution
583 Standardized Precipitation Evapotranspiration Index (SPEI) dataset for Africa, Centre for Environmental Data Analysis, doi:
584 10.5285/bbdfd09a04304158b366777eba0d2aeb. , 2019a. 2019a.

585 Peng, J., Dadson, S., Leng, G., Duan, Z., Jagdhuber, T., Guo, W., and Ludwig, R.: The impact of the Madden-Julian Oscillation on
586 hydrological extremes, *Journal of Hydrology*, 571, 142-149, 2019c.

587 Peng, J., Muller, J.-P., Blessing, S., Giering, R., Danne, O., Gobron, N., Kharbouche, S., Ludwig, R., Müller, B., and Leng, G.:
588 Can We Use Satellite-Based FAPAR to Detect Drought?, *Sensors*, 19, 3662, 2019d.

589 Pinzon, J. E. and Tucker, C. J.: A non-stationary 1981–2012 AVHRR NDVI3g time series, *Remote Sensing*, 6, 6929-6960, 2014.

590 Pozzi, W., Sheffield, J., Stefanski, R., Cripe, D., Pulwarty, R., Vogt, J. V., Heim Jr, R. R., Brewer, M. J., Svoboda, M., and
591 Westerhoff, R.: Toward global drought early warning capability: Expanding international cooperation for the development of a
592 framework for monitoring and forecasting, *Bulletin of the American Meteorological Society*, 94, 776-785, 2013.

593 Richard, W., Sonia, I. S., Martin, H., Jinfeng, C., Philippe, C., Delphine, D., Joshua, E., Christian, F., Simon, N. G., Lukas, G.,
594 Alexandra-Jane, H., Thomas, H., Akihiko, I., Nikolay, K., Hyungjun, K., Guoyong, L., Junguo, L., Xingcai, L., Yoshimitsu, M.,
595 Catherine, M., Christoph, M., Hannes Müller, S., Kazuya, N., Rene, O., Yadu, P., Thomas, A. M. P., Yusuke, S., Sibyll, S., Erwin,
596 S., Justin, S., Tobias, S., Joerg, S., Qihong, T., Wim, T., Yoshihide, W., Xuhui, W., Graham, P. W., Hong, Y., and Tian, Z.:
597 Evapotranspiration simulations in ISIMIP2a—Evaluation of spatio-temporal characteristics with a comprehensive ensemble of
598 independent datasets, *Environmental Research Letters*, 13, 075001, 2018.

599 Rivera, J. A., Marianetti, G., and Hinrichs, S.: Validation of CHIRPS precipitation dataset along the Central Andes of Argentina,
600 *Atmospheric Research*, 213, 437-449, 2018.

601 Rojas, O., Vrieling, A., and Rembold, F.: Assessing drought probability for agricultural areas in Africa with coarse resolution
602 remote sensing imagery, *Remote sensing of Environment*, 115, 343-352, 2011.

603 Schneider, U., Ziese, M., Meyer-Christoffer, A., Finger, P., Rustemeier, E., and Becker, A.: The new portfolio of global
604 precipitation data products of the Global Precipitation Climatology Centre suitable to assess and quantify the global water cycle
605 and resources, *Proceedings of the International Association of Hydrological Sciences*, 374, 29-34, 2016.

606 Schwalm, C. R., Anderegg, W. R. L., Michalak, A. M., Fisher, J. B., Biondi, F., Koch, G., Litvak, M., Ogle, K., Shaw, J. D., Wolf,
607 A., Huntzinger, D. N., Schaefer, K., Cook, R., Wei, Y., Fang, Y., Hayes, D., Huang, M., Jain, A., and Tian, H.: Global patterns of
608 drought recovery, *Nature*, 548, 202, 2017.

609 Sheffield, J., Wood, E. F., Chaney, N., Guan, K., Sadri, S., Yuan, X., Olang, L., Amani, A., Ali, A., and Demuth, S.: A drought
610 monitoring and forecasting system for sub-Sahara African water resources and food security, *Bulletin of the American
611 Meteorological Society*, 95, 861-882, 2014.

612 Shukla, S., McNally, A., Husak, G., and Funk, C.: A seasonal agricultural drought forecast system for food-insecure regions of
613 East Africa, *Hydrology and Earth System Sciences*, 18, 3907-3921, 2014.

614 Spinoni, J., Naumann, G., Vogt, J. V., and Barbosa, P.: The biggest drought events in Europe from 1950 to 2012, *Journal of
615 Hydrology: Regional Studies*, 3, 509-524, 2015.

616 Sun, Q., Miao, C., AghaKouchak, A., and Duan, Q.: Century-scale causal relationships between global dry/wet conditions and the
617 state of the Pacific and Atlantic Oceans, *Geophysical Research Letters*, 43, 6528-6537, 2016a.

618 Sun, S., Chen, H., Li, J., Wei, J., Wang, G., Sun, G., Hua, W., Zhou, S., and Deng, P.: Dependence of 3-month Standardized
619 Precipitation-Evapotranspiration Index dryness/wetness sensitivity on climatological precipitation over southwest China,
620 *International Journal of Climatology*, 38, 4568-4578, 2018.

621 Sun, S., Chen, H., Wang, G., Li, J., Mu, M., Yan, G., Xu, B., Huang, J., Wang, J., and Zhang, F.: Shift in potential
622 evapotranspiration and its implications for dryness/wetness over Southwest China, *Journal of Geophysical Research:
623 Atmospheres*, 121, 9342-9355, 2016c.

624 Swain, D. L., Tsiang, M., Haugen, M., Singh, D., Charland, A., Rajaratnam, B., and Diffenbaugh, N. S.: The extraordinary
625 California drought of 2013/2014: Character, context, and the role of climate change, *Bull. Am. Meteorol. Soc*, 95, S3-S7, 2014.

626 Törnros, T. and Menzel, L.: Addressing drought conditions under current and future climates in the Jordan River region,
627 *Hydrology and Earth System Sciences*, 18, 305-318, 2014.

628 Toté, C., Patricio, D., Boogaard, H., Van Der Wijngaart, R., Tarnavsky, E., and Funk, C.: Evaluation of satellite rainfall estimates
629 for drought and flood monitoring in Mozambique, *Remote Sensing*, 7, 1758-1776, 2015.

630 Trambauer, P., Dutra, E., Maskey, S., Werner, M., Pappenberger, F., Van Beek, L., and Uhlenbrook, S.: Comparison of different
631 evaporation estimates over the African continent, *Hydrology and Earth System Sciences*, 18, 193-212, 2014.

632 Trambauer, P., Maskey, S., Winsemius, H., Werner, M., and Uhlenbrook, S.: A review of continental scale hydrological models
633 and their suitability for drought forecasting in (sub-Saharan) Africa, *Physics and Chemistry of the Earth, Parts A/B/C*, 66, 16-26,
634 2013.

635 Um, M.-J., Kim, Y., Park, D., and Kim, J.: Effects of different reference periods on drought index (SPEI) estimations from 1901 to
636 2014, *Hydrology & Earth System Sciences*, 21, 2017.

637 van der Schrier, G., Barichivich, J., Briffa, K., and Jones, P.: A scPDSI-based global data set of dry and wet spells for 1901–2009,
638 *Journal of Geophysical Research: Atmospheres*, 118, 4025-4048, 2013.

639 van Dijk, A. I., Beck, H. E., Crosbie, R. S., de Jeu, R. A., Liu, Y. Y., Podger, G. M., Timbal, B., and Viney, N. R.: The
640 Millennium Drought in southeast Australia (2001–2009): Natural and human causes and implications for water resources,
641 ecosystems, economy, and society, *Water Resources Research*, 49, 1040-1057, 2013.

642 Van Loon, A. F.: *Hydrological drought explained*, Wiley Interdisciplinary Reviews: Water, 2, 359-392, 2015.

643 Vicente-Serrano, S.: Foreword: Drought complexity and assessment under climate change conditions, *Cuadernos de Investigación
644 Geográfica*, 42, 7-11, 2016.

645 Vicente-Serrano, S. M.: Evaluating the impact of drought using remote sensing in a Mediterranean, semi-arid region, *Natural*
646 *Hazards*, 40, 173-208, 2007.

647 Vicente-Serrano, S. M. and Beguería, S.: Comment on ‘Candidate distributions for climatological drought indices (SPI and SPEI)’
648 by James H. Stagge et al, *International Journal of Climatology*, 36, 2120-2131, 2016.

649 Vicente-Serrano, S. M., Beguería, S., Gimeno, L., Eklundh, L., Giuliani, G., Weston, D., El Kenawy, A., López-Moreno, J. I.,
650 Nieto, R., and Ayenew, T.: Challenges for drought mitigation in Africa: The potential use of geospatial data and drought
651 information systems, *Applied Geography*, 34, 471-486, 2012a.

652 Vicente-Serrano, S. M., Beguería, S., and López-Moreno, J. I.: A multiscalar drought index sensitive to global warming: the
653 standardized precipitation evapotranspiration index, *Journal of climate*, 23, 1696-1718, 2010.

654 Vicente-Serrano, S. M., Beguería, S., Lorenzo-Lacruz, J., Camarero, J. J., López-Moreno, J. I., Azorin-Molina, C., Revuelto, J.,
655 Morán-Tejeda, E., and Sanchez-Lorenzo, A.: Performance of Drought Indices for Ecological, Agricultural, and Hydrological
656 Applications, *Earth Interactions*, 16, 1-27, 2012b.

657 Vicente-Serrano, S. M., García-Herrera, R., Barriopedro, D., Azorin-Molina, C., López-Moreno, J. I., Martín-Hernández, N.,
658 Tomás-Burguera, M., Gimeno, L., and Nieto, R.: The Westerly Index as complementary indicator of the North Atlantic oscillation
659 in explaining drought variability across Europe, *Climate Dynamics*, 47, 845-863, 2016.

660 Vicente-Serrano, S. M., Gouveia, C., Camarero, J. J., Beguería, S., Trigo, R., López-Moreno, J. I., Azorín-Molina, C., Pasho, E.,
661 Lorenzo-Lacruz, J., Revuelto, J., Morán-Tejeda, E., and Sanchez-Lorenzo, A.: Response of vegetation to drought time-scales
662 across global land biomes, *Proceedings of the National Academy of Sciences*, 110, 52-57, 2013.

663 Vicente-Serrano, S. M., Miralles, D. G., Domínguez-Castro, F., Azorin-Molina, C., Kenawy, A. E., McVicar, T. R., Tomás-
664 Burguera, M., Beguería, S., Maneta, M., and Peña-Gallardo, M.: Global Assessment of the Standardized Evapotranspiration
665 Deficit Index (SEDI) for Drought Analysis and Monitoring, *Journal of Climate*, 31, 5371-5393, 2018.

666 Vicente-Serrano, S. M., Tomás-Burguera, M., Beguería, S., Reig, F., Latorre, B., Peña-Gallardo, M., Luna, M. Y., Morata, A., and
667 González-Hidalgo, J. C.: A high resolution dataset of drought indices for Spain, *Data*, 2, 22, 2017.

668 von Hardenberg, J., Meron, E., Shachak, M., and Zarmi, Y.: Diversity of vegetation patterns and desertification, *Physical Review*
669 *Letters*, 87, 198101, 2001.

670 Wang, H. and He, S.: The North China/Northeastern Asia Severe Summer Drought in 2014, *Journal of Climate*, 28, 6667-6681,
671 2015.

672 Wegren, S. K.: Food security and Russia's 2010 drought, *Eurasian Geography and Economics*, 52, 140-156, 2011.

673 Wilhite, D. and Pulwarty, R.: Drought as Hazard: Understanding the Natural and Social Context. In: *Drought and Water Crises:*
674 *Integrating Science, Management, and Policy*, 2017.

675 Wilhite, D. A., Svoboda, M. D., and Hayes, M. J.: Understanding the complex impacts of drought: A key to enhancing drought
676 mitigation and preparedness, *Water resources management*, 21, 763-774, 2007.

677 Xu, Y., Wang, L., Ross, K. W., Liu, C., and Berry, K.: Standardized Soil Moisture Index for Drought Monitoring Based on Soil
678 Moisture Active Passive Observations and 36 Years of North American Land Data Assimilation System Data: A Case Study in the
679 Southeast United States, *Remote Sensing*, 10, 301, 2018.

680 Yuan, X., Wood, E. F., Chaney, N. W., Sheffield, J., Kam, J., Liang, M., and Guan, K.: Probabilistic Seasonal Forecasting of
681 African Drought by Dynamical Models, *Journal of Hydrometeorology*, 14, 1706-1720, 2013.

682 Zambrano-Bigiarini, M., Nauditt, A., Birkel, C., Verbist, K., and Ribbe, L.: Temporal and spatial evaluation of satellite-based
683 rainfall estimates across the complex topographical and climatic gradients of Chile, *Hydrology and Earth System Sciences*, 21,
684 1295-1320, 2017.

685 Zhan, S., Song, C., Wang, J., Sheng, Y., and Quan, J.: A global assessment of terrestrial evapotranspiration increase due to surface
686 water area change, *Earth's future*, 7, 266-282, 2019.

687 Zhao, M., A. G., Velicogna, I., and Kimball, J. S.: A Global Gridded Dataset of GRACE Drought Severity Index for 2002–14:
688 Comparison with PDSI and SPEI and a Case Study of the Australia Millennium Drought, *Journal of Hydrometeorology*, 18, 2117-
689 2129, 2017.

690 Zhou, Q., Leng, G., and Peng, J.: Recent Changes in the Occurrences and Damages of Floods and Droughts in the United States,
691 *Water*, 10, 1109, 2018.

692 Ziese, M., Schneider, U., Meyer-Christoffer, A., Schamm, K., Vido, J., Finger, P., Bissolli, P., Pietzsch, S., and Becker, A.: The
693 GPCC Drought Index—a new, combined and gridded global drought index, *Earth System Science Data*, 6, 285-295, 2014.

694

695